High Efficiency and Low Photodegradation in Random Laser, using Novel TiO$_2$@Silica Nanoparticles

Ernesto Jimenez-Villar[1,2], Valdeci Mestre[3], Paulo C. De Oliveira[3],
Wagner M. Faustino[4] and Gilberto F. De Sá[1]

[1]*Departamento de Química Fundamental, Universidade Federal de Pernambuco, Recife, PE,50670-901, Brazil*
[2]*Instituto de Ciencia Molecular, Universitat de València. C/ Catedrático José Beltrán Nº 2, 46980 Paterna Valencia, Spain*
[3]*Departamento de Física, Universidade Federal da Paraíba, João Pessoa, Paraíba 580051-970, Brazil*
[4]*Departamento de Química, Universidade Federal da Paraíba, João Pessoa, Paraíba 58051-970, Brazil*

Keywords: Core-Shell Nanoparticles, Random Laser, TiO$_2$@Silica Nanoparticles, TiO$_2$ Dye Photodegradation.

Abstract: Here we have studied a novel scattering medium for random laser. This medium is composed of TiO$_2$@Silica nanoparticles suspended in an ethanol solution of rhodamine 6G. TiO$_2$ nanoparticles with average diameter of 0.41 μm were coated with a silica shell of ~40 nm thickness. Random laser study comparing TiO$_2$ and TiO$_2$@Silica nanoparticles suspended in ethanol solution of rhodamine 6G was performed. The study showed a high efficiency, low threshold, narrower bandwidth and lower photodegradation for TiO$_2$@Silica system. Optical and chemical stability has been combined by coating TiO$_2$ nanoparticles with a silica shell of ~40nm thickness.

1 INTRODUCTION

The first evidence of random laser (RL) in solution was obtained by Lawandy et. al. (Lawandy, 1994) who suspended TiO$_2$ nanoparticles (Np) in a conventional laser dye. RL action have been observed in a variety of gain media including polymeric films with and without intentionally introduced scatterers (Polson, 2001), in GaN nanocolumns (Masaru, 2010), dye-infiltrated opals (Shkunov, 2001), porous media infiltrated with liquid crystals with dyes (Wiersma, 2001), porous network of air into a solid glass or semiconductor crystal (Schuurmans, 1999), ZnO scattering films and nanoclusters (Cao, 2001), on waveguided plasmonic (Tianrui, 2011) and many others. In the works reported by Noginov (Noginov, 2005), Cao (Cao, 2005) and Wiersma (Wiersma, 2008) detailed reviews on RL can be found.

The strategy introduced by Lawandy, suspending highly scattering particles in laser dye has been repeated by other authors (Noginov, 1995), (Leonetti, 2012) in order to study the random laser. However, the photodegradation effect and the inability to ensure complete colloidal dispersion, have limited the development and applications of such systems. The complete colloidal dispersion is related to an increase of the scattering surface per unit volume with the suspended particles concentration. This is extremely difficult to obtain in solution at high concentrations, because particles tend to agglomerate (Mandzy, 2005). The surface modification of TiO$_2$ Np with a silane coupling agent has been used in order to reduce the agglomeration effect and improve the mechanical properties and UV protection of urethane clear coatings in TiO$_2$ composites (Sabzi, 2009). Other authors have reported the replacement of the dispersive medium (TiO$_2$ Np) by silica Np (Brito-Silva, 2010), demonstrating random lasing. This kind of scattering medium greatly decreases the photodegradation effect. However, the relatively small difference in refractive index between silica and the alcohol-dye solution in comparison to TiO$_2$ causes a threshold increase and an efficiency decrease of the RL. In this work, we propose to study photodegradation effect and action of RL composed of TiO$_2$@Silica particles suspended in ethanol solution of rhodamine 6G (R6G). Particles like TiO$_2$@SiO$_2$ have already been synthesized before (over ten years back) (Joseph, 2000), however, their application in RL has been done very recently (Jimenez-Villar, 2013), (B-Jimenez-Villar,

2013). In this work, we have studied the RL action and Photodegradation effect for an extended range of pumping energy fluencies (between 0.12 and 264 mJ/cm^2).

The silica shell with thickness around 40 nm presents a steric effect, preventing the "optical" junction of scattering TiO_2 surfaces. Moreover, this silica shell should improve the light coupling with the TiO_2 particles by light refraction at the ethanol-silica interface. In addition, silica shell acts as a barrier to prevent the charge transfer, which is the principal cause of the dye degradation (Fox, 1993). These have been practical difficulties for the development of RL and novel optical devices with improved performance and functionality. In turn, the silica coating is particularly advantageous due to its high dispersibility (Jimenez, 2008), (Jimenez, 2010), low density, and the inertness of nanoparticles (Fuertes, 2011), (B-Fuertes, 2011) along with the numerous possibilities for their use, (Rodriguez, 2005), (Rodriguez, 2008).

Therefore strongly scattering particles coated with a shell of thickness and refractive index suitable could open new opportunities to achieve significant improvements in the operation of RL and photonic devices based on highly disordered scattering media.

2 EXPERIMENTAL SECTION

2.1 Chemical Synthesis and Characterization

Rhodamine 6G laser dye ($C_{28}H_{31}N_2O_3Cl$) with molecular weight 479.02 g/mol supplied by Fluka: Ethanol alcohol (C_2H_5OH) with spectroscopic grade purity supplied by Alphatec: Tetra-ethyl-ortho-silicate (TEOS) supplied by Sigma-Aldrich. Titanium dioxide (TiO_2 Np; diameter 410 nm) of rutile crystal structure was acquired from DuPont Inc (R900).

Two kinds of samples were prepared containing [$1x10^{-4}$ M] of Rhodamine 6G (R6G), one with TiO_2 and another with TiO_2@Silica scatters Np. The silica coating of TiO_2 Np was made via Stöber method (Stöber, 1968), (Sheng-Li, 1997), (Abderrafi, 2012). In the first stage 2 g of TiO_2 Np were dispersed in 250 ml of absolute ethanol by ultrasound bath for 20 minutes. Then, the solution of TiO_2 Np was divided into two equal portions of 125 ml. One of the parts was placed in a bath at 5 °C and 1.1 ml of TEOS, previously diluted in 11 ml of ethanol, was added. The 10% diluted solution of TEOS was added in 110

portions of 100 µl during the course of 1 hour. The solution was stirred during the TEOS addition and after it was stored during 4 week at room temperature. The other portion was stored and used as a reference in every experiment.

The silica coating on the TiO_2 Np were examined by transmission electron microscopy (TEM), performed on a 100 kV JEOL, model 1200EX, microscope. The commercial carbon-coated Cu TEM grid was immersed in the solution of TiO_2@Silica Np previously diluted 50-fold lower and then left to dry before being introduced into the microscope. The stoichiometric ratio (Ti/Si) of nanoparticles (TiO_2@Silica) was determined by Energy Dispersive X-Ray fluorescence (ED-XRF) using an X-ray spectrometer SIEMENS D5000. The sample was prepared in three steps; precipitation, washing and drying. The nanoparticles powder (TiO_2@Silica) was pressed into a tablet form of a 12mm diameter for analysis.

2.2 Experimental Setup of Random Laser

Figure 1C shows a schematic diagram of the RL experimental setup. The pumping source was the second harmonic of a Q-switched Nd: YAG Continuum Minilite II (25 mJ, λ = 532 nm, with a pulse width of ~6 ns, repetition rate up to 15 Hz, and spot size of 3 mm). The laser power was regulated through neutral density filters (NDF), a polarizer and a half wave plate. The samples were accommodated in a 2 mm pathlength quartz cuvette. The pump laser beam was incident upon the sample at 15 deg. The emission spectra were collected through a multimode optical fiber (200 µm) coupled to a spectrometer HR4000 UV-VIS (Ocean Optics) with 0.36 nm spectral resolution (FWHM). The collection angle (optical fiber) was ~45 deg with respect to the incident pumping beam, that is, 60 deg with respect to the cuvette surface. The liquid samples were placed in an ultrasound bath for about 10 minutes before recording the spectrum, in order to obtain the same dispersion of nanoparticles (initial conditions) in all measurements.

3 RESULTS AND DISCUSSION

3.1 Silica Shell onto TiO_2 Nanoparticles

In TEM images (Figure 1A) we observe the silica coating on TiO_2 Np, such as the one indicated by the

yellow arrows. This silica shell presents an irregular morphology with a thickness ranging between 20 nm and 70 nm. Figure 1B shows the surface of one TiO_2 Np, before the coating with silica. As can be seen, the Np surface is irregular; this fact should determine the morphology of the silica coating subsequently. The mass percentage ratio (Ti/Si) determined by ED-XRF was Ti_{70}/Si_{30}. The average thickness of silica coating, calculated from the typical silica density obtained by the TEOS hydrolysis 2.1 g/cm³ (Karmakar, 2000), was ~40 nm. In this way, the silica shell represents a barrier that prevents the "optical" binding of TiO_2 scattering surfaces, with the additional advantage to present a chemically stable surface (SiO_2).
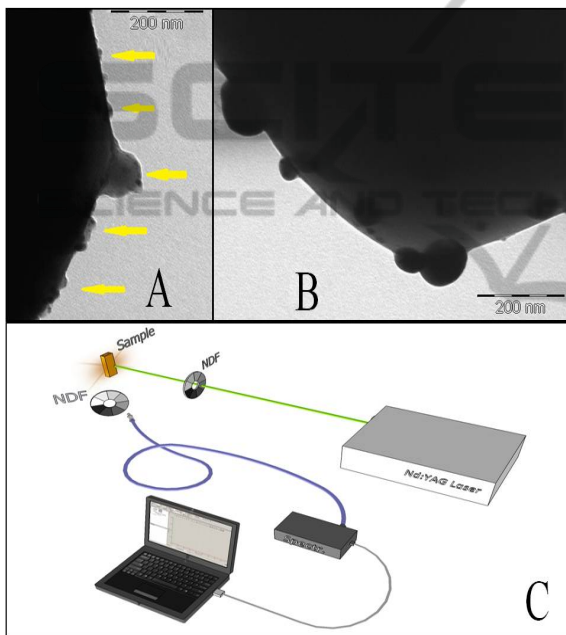

Figure 1: TEM images of; A) silica coating on the TiO_2@Silica surface and B) TiO_2 nanoparticle surface. The scale bars represent 200 nm. Yellow arrows (A) indicate the silica coating. C) Schematic diagram of the RL experimental setup.

3.2 Random Laser Action

Figures 2A and 2B show the behaviour of the emitted intensity and the spectral width (FWHM), as a function of pumping energy fluencies for the two kind of scattering medium (TiO_2 and TiO_2@Silica). The RL action for pumping energy fluencies between 0.12 and 264 mJ/cm² were performed. The calculated concentrations of scatters Np and dye were 5.6 x10¹⁰ Np/ml and 1x10⁻⁴ M, respectively. Each value of emission intensity and bandwidth represented in the graphs (fig. 2A and B) was taken

by integrating 10 laser pulses, which allowed us to rule out any photodegradation effects during the measurement. As observed, the RL action for TiO_2@Silica system is improved, i.e. presented higher slope efficiency, narrower bandwidth and lower laser threshold. For the TiO_2@Silica system, the laser slope efficiency was ~2.1 times greater than for TiO_2.

The RL threshold values extracted from the fittings (fig.2B) for TiO_2 and TiO_2@Silica systems were 2.29 ±0.04 mJ/cm² and 1.79 ±0.02 mJ/cm², respectively. The highest gain narrowing factor, defined as the FWHM of the emitted light below threshold divided by the FWHM of the emission spectrum of the RL far above threshold gave a value of 12.2 for TiO_2@Silica, and 10.6 for TiO_2, which corresponds to β-factors (Gijs van Soest, 2002) of 0.082 e 0.094 respectively.

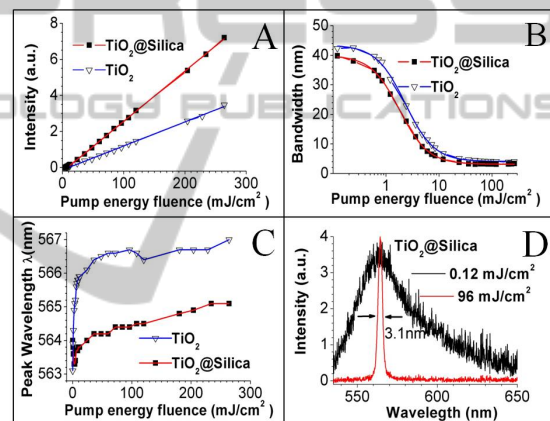Figure 2: A) The emitted peak intensity and B) spectral FWHM emission of the RL, for the two kinds of nanoparticles (TiO_2 and TiO_2@Silica). The solid lines represent the fits with experiments points; blue and red lines correspond to the TiO_2 and TiO_2@Silica systems, respectively. C) Influence of the pump energy fluence on peak wavelength of emission spectrums for TiO_2 and TiO_2@Silica systems. D) (Black online) Emission spectra below (broad band spectrum) and above (narrow band spectrum) the RL threshold for TiO_2@Silica system.

The peak position of the emission spectrum was measured as a function of the pumping energy fluence (between 0.12 and 260 mJ/cm²). Figure 2c shows a comparison of these peak positions with fluence for the TiO_2@Silica and TiO_2 systems. The emission spectrum shows a redshift for the TiO_2 system, which undergoes a large increase in fluencies between 0.12 and 12 mJ/cm² (0 to 2.8 nm). This redshift increases (between 3 and 3.9 nm) for fluencies >12 mJ/cm². This shift was previously observed and explained by a model considering

absorption and emission at the transition between the ground and the first excited singlet of the dye molecule (Noginov. 1995). Instead, the emission spectrum peak for TiO$_2$@Silica system shows a blueshift for fluencies ≤12 mJ/cm^2. For fluencies between 12 mJ/cm^2 and 260 mJ/cm^2, the redshift increases in the same fashion, from 0 up to ~1 nm. A comparison between the emission spectra of the TiO$_2$@Silica system for fluencies well below (0.12 mJ/cm^2) and far above RL threshold (96 mJ/cm^2) is showed in the figures 2D. The peaks intensities of the narrow and broad bands were normalized to show the narrowing effect more clearly. The peak intensity relationship (narrow/broad) is ~4 orders magnitude larger. The redshift of the RL spectrum is almost null (<0.5nm) at this fluence (96 mJ/cm^2). This effect should be due to the fact that the ratio between R6G molecules and R6G molecules involved in the stimulated emission is close to unit [R6G]/[R6G$_{stimulated}$]≈1 at 96mJ/cm^2, which is evidenced in a higher efficiency of the RL (TiO$_2$@Silica). The above results could be explained by the increase of effective scattering surface per unit volume due to the "optical" colloidal stability and light coupling enhancement with TiO$_2$ scattering cores provided by the silica shell. It is known that silica Np have a higher colloidal stability than those of TiO$_2$ (Yang. 2008), (Chih-ping, 2010). In this way, the scattering mean free path (l_s) should be lower for TiO$_2$@Silica system, which mean that pumping energy is confined in a lower volume. Furthermore, the amount of R6G molecules inside the excited volume is lower, being able to excite a higher percentage of molecules. The scattering mean free path measured for TiO$_2$ and TiO$_2$@Silica systems were 52 ±4μm and 20.6 ±0.2μm, respectively (Jimenez-Villar, 2013). Notice that, the volume of emission laser should increase with pumping fluence (I_{P0}). The pumping fluence at a depth length l inside the scattering medium (I_{Pl}) could be expressed as follows:

$$I_{Pl} = I_{P0}\left(e^{-l/l_s} + e^{-l/l_a}\right) \qquad (1)$$

l_a is the ballistic absorption length. The diffuse intensity has been neglected. When $l_s \ll l_a$,

$$I_{Pl} = I_{P0}e^{-l/l_s} \qquad (2)$$

Therefore, there would be a limit depth length (l_T) inside the scattering medium, beyond which the pumping intensity (I_{PT}) is unable to provoke population inversion. The l_T should depend on the pumping fluence I_{P0} as follows:

$$I_{PT} = I_{P0}e^{-l_T/l_s} \to l_T = l_s * (\ln I_{P0} - \ln I_{PT}) \qquad (3)$$

I_{PT} would correspond with the RL threshold fluence. Therefore, for $I_{P0} \gg I_{PT}$ then l_T is directly proportional to l_s. In turn, the effective pumping intensity into the RL emission region is inversely proportional to l_s, so, it should be higher for TiO$_2$@Silica system.

Figure 3 shows a RL representative scheme consisting of a TiO$_2$@Silica Nps suspension in an ethanol solution of R6G. The silica shell avoids the contact between TiO$_2$ scattering surfaces, leading to a scattering area per unit volume higher and consequently to an increase of scattering strength.
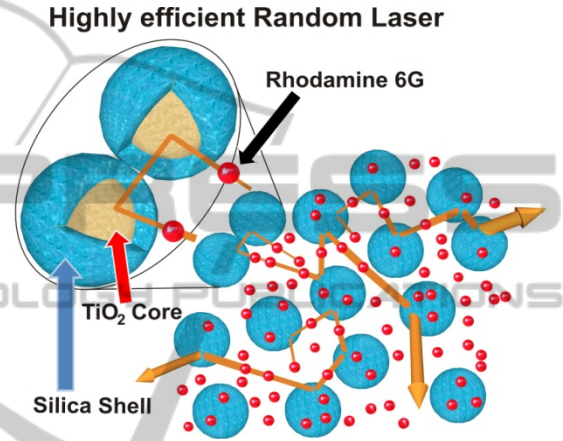

Figure 3: Representative scheme of the random laser, it consists of a TiO$_2$@Silica Nps suspension in an ethanol solution of R6G. The blue coating represents the silica shell on the TiO$_2$ Nps and the little red spheres correspond to the R6G molecules. The silica shells between two TiO$_2$ cores lead to a scattering strength increasing.

3.3 Photodegradation Study

Figure 4 shows the photodegradation process by the RL emission intensity as a function of shots number for systems TiO$_2$ (A) and TiO$_2$@Silica (B). The laser beam of 3 mm diameter and fluencies of 200 mJ/cm^2 and 260 mJ/cm^2, was used to pump the samples, which volume was 200 μl accommodated in a 2 mm pathlength quartz cuvette. Fig. 3A and 3B show a decrease in emission intensity (RL) with the number of shots for the pumping fluencies 200 mJ/cm^2(red) and 260 mJ/cm^2 (black). The TiO$_2$ system shows a rapid exponential decay. The number of shots for which the emission intensity decreases to 50% for the fluencies of 200 and 260 mJ/cm^2 was 960 and 342, respectively. However, for the TiO$_2$@Silica system the number of shots required were much higher, 59077 (200 mJ/cm^2) and 26010 (260 mJ/cm^2), respectively. These represent a decrease in the photodegradation rate more than 60

times (200 mJ/cm^2) and 74 times (260 mJ/cm^2), respectively.

The TiO$_2$ photocatalytic properties are a well studied subject, which has been used to remove or degrade dyes from the environment (G. van, 1993). The photocatalytic pathway involves a reaction on the TiO$_2$ surface following several steps: 1) photogeneration of electron–hole pairs by exciting the semiconductor with >3.2 eV light; 2) separation of electrons and holes by traps existing on the TiO$_2$ surface; 3) a redox process induced by the separated electrons and holes with the adsorbates present on the surface.
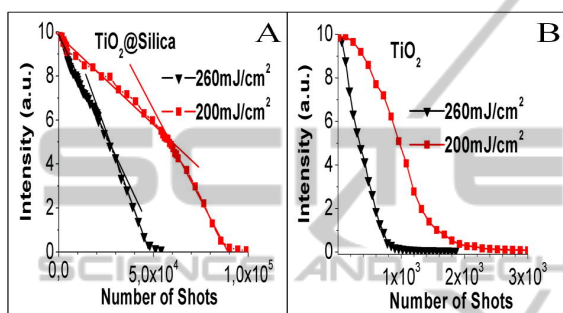

Figure 4: A-B) Photodegradation process of Random laser action as a function of the number of shots for the laser pumping fluencies of 200 mJ/cm^2 (red) and 260 mJ/cm^2 (black): A) TiO$_2$ Np system; B) TiO$_2$@Silica Np system.

The exponential decrease of the RL intensity, for the system TiO$_2$, indicates that the photodegradation is proportional to its derivative, as to the photodegradation rate. This means that the charge transfers (Amy, 1995) and therefore the redox reaction (Serpone, 1989) will cause a greater charge transfer in the next laser shot. Thus, one might think that the high concentrations of charges created by the TiO$_2$ nanoparticles at high pumping fluencies must react with the proper surface of the nanoparticles, reducing Ti^{4+} and oxidizing O^{2-}. This process results in oxygen vacancies (Tsukamoto, 2008), which act as traps for photoelectrons. These electrons, trapped near the surface, act as a source of electron transfer coming from these superficial traps, increasing the efficiency of the redox process (Heinz, 1991). Additionally, the creation of oxygen vacancies in TiO$_2$ causes a progressive decreasing of gap on the nanoparticle surfaces (TiO$_2$), which is reflected in the progressive increase in the creation of electron-hole pairs. This photo-darkening effect is observed in films of TiO$_2$ exposed to successive irradiation of laser pulses (Tsukamoto, 2011), (Tsukamoto, 2008).

The photodegradation process for the TiO$_2$@Silica system presents a linear behaviour. However, the modulus of the slope increases slightly after the emission intensity decreases to 50%. Subsequently, the photodegradation rate experiences a slight increase, but remains constant. This phenomenon could be due to the decreased absorption of R6G, provoking an increase of the effective pumping fluence inside the scattering medium (TiO$_2$@Silica), which should increase the photodegradation rate of R6G.

The photodegradation process (RL) for the system TiO$_2$@Silica could be explained through the reaction of the ethanol radical CH$_3$CHOH with R6G ground state molecules (Adrian, 1976). The free radical CH$_3$CHOH is produced by energy transfer from the R6G molecules in a higher triplet state, which is produced by two sequential single-photon absorptions (Yamashita, 1976). This photodegradation process is much less effective, since it does not involve charges transfer from the TiO$_2$ nanoparticles, which is known as an efficient photocatalyzers.

4 CONCLUSIONS

The RL action using a novel scattering media composed by titanium oxide Np coated with ~40nm thickness of silica shell was studied. This scattering medium (TiO$_2$@Silica Np) combine the high refractive index of TiO$_2$ with chemical inertness, "optical" colloidal stability and light coupling enhancement (TiO$_2$ cores) provided by the silica shell. Random lasing with higher efficiency, lower threshold, narrower bandwidth and very long photo-bleaching lifetime was obtained. The RL efficiency was 2.1 times higher and the R6G photodegradation period was between 60 and 74 times higher than the conventional scattering medium (TiO$_2$). The high RL efficiency was ascribed to lower l_s for TiO$_2$@Silica system. This fact is associated with the silica shell, which avoid the "optical" junction of TiO$_2$ scattering surface and improves the light coupling with TiO$_2$ cores. In other words, the core-shell scattering particles present a core with high refractive index (TiO$_2$) and a shell that combines high chemical stability, light coupling enhancement (TiO$_2$ cores) and a steric "optical" effect. Therefore, a lower l_s provokes higher effective pumping fluence, leading to higher population inversion and stimulated emission rate. In this way, it has been remarked the colloidal stability of the scattering

medium, which is an important parameter and is not insignificant for the treatment of RL.

The lower photodegradation period was associated to the higher chemical stability provided by the silica shell, which should establish a potential barrier for the charge transfer.

ACKNOWLEDGEMENTS

REFERENCES

Lawandy, N. M., Balachandran, R. M., Gomes, A. S. L. & Sauvain, E., 1994. *Nature, 368*, 436–438.

Polson R. C., Chipoline A. and Vardeny Z. V., 2001. *Advanced Materials, 13*, 760-764.

Masaru Sakai, Yuta Inose, Kazuhiro Ema, Tomi Ohtsuki, Hiroto Sekiguchi, Akihiko Kikuchi, and Katsumi Kishino, 2010. *Appl. Phys. Lett.*, 97, 151109.

M. N. Shkunov, M. C. DeLong, M. E. Raikh, Z. V. Vardeny, A. A. Zakhidov and R. H. Baughman, *Synthetic Metals,* 2001, *116*, 485-491.

Wiersma D. and Cavalier S., 2001. *Nature, 414*, 708-709.

Schuurmans, F. J. P., Vanmaekelbergh, D., van de Lagemaat, J. & Lagendijk, A. 1999. *Science, 284*, 141–143.

Cao H., Ling Y., Xu J. Y., Cao C. Q. and Kumar P., 2001. *Phys. Rev. Lett., 86*, 4524-4527.

Tianrui Zhai, Xinping Zhang, Zhaoguang Pang, Xueqiong Su, Hongmei Liu, Shengfei Feng, and Li Wang, 2011. *Nano Lett., 11* (10), 4295–4298.

Noginov M. A., 2005. "Solid-State Random Lasers," (Springer Series in Optical Sciences), Norfolk State University, Norfolk.

Hui Cao, 2005. *J. Phys. A: Math. Gen.*, *38*, 10497–10535.

Wiersma D. S., 2008. *Nature Physics, 4*, 359-367.

Sha W., Liu C.-H., and Alfano R., 1994. *J.Opt. Soc. Amer., B 19*, 1922–1924.

Noginov M. A., Caulfield H. J., Noginova N. E., and Venkateswarlu P., 1995. *Opt. Commun., 118*, 430–437.

Leonetti M., Conti C. and Cefe Lopez, 2012. *Appl. Phys. Lett., 101*, 051104.

Mandzy N., Grulke E., Druffel T., 2005. *Powder Technology, 160*, 121–126.

Sabzi M., Mirabedini S.M., Zohuriaan-Mehr J., Atai M., 2009. *Progress in Organic Coatings, 65*, 222–228.

Brito-Silva A. M., André Galembeck, Anderson S. L. Gomes, Alcenisio Jesus-Silva J., Cid B. de Araújo, 2010. *Journal of Applied Physics, 108*, 033508.

Joseph N. Ryan , Menachem Elimelech , Jenny L. Baeseman , Robin D. Magelky, 2000. *Environ. Sci. Technol.*, *34*, 2000-2005.

E. Jimenez-Villar, Valdeci Mestre, Paulo C. de Oliveira, Gilberto F. de Sá, 2013. *Nanoscale*, in press; DOI:10.1039/C3NR03603K.

B-E. Jimenez-Villar, Valdeci Mestre, Paulo C. de Oliveira, Wagner M. Faustino, D. S. Silva, Gilberto F. de Sá, 2013, *Appl. Phys, Lett.*, *Submitted*.

Fox M. A., Dulay M. T., 1993. *Chem. Rev., 93*, 341.

E. Jimenez, Kamal Abderrafi, Juan Martınez-Pastor, Rafael Abargues, Jose Luıs Valdes, Rafael Ibañez, 2008. *Superlattices and Microstructures, 43*, 487–493.

Ernesto Jimenez, Kamal Abderrafi, Rafael Abargues, Jose L. Valdes, Juan P. Martınez-Pastor, 2010. *Langmuir, 26* (10), 7458–7463.

Gustavo Fuertes, Orlando L. Sanchez-Munoz, Esteban Pedrueza, Kamal Abderrafi, Jesus Salgado, Ernesto Jimenez, 2011. *Langmuir, 27*, 2826–2833.

B-Gustavo Fuertes, Esteban Pedrueza, Kamal Abderrafi, Rafael Abargues, Orlando Sánchez, Juan Martínez-Pastor, Jesús Salgado, Ernesto Jiménez, 2011. *Proc. SPIE Medical Laser Applications and Laser-Tissue Interactions V*, No. 8092-51.

Rodriguez E., Jimenez E., Jacob G. J., Neves A. A. R., Cesar C. L., Barbosa L. C., 2005. *Physica E, 26*, 361.

Rodriquez E., Kellerman G., Jiménez E., César C. L., Barbosa L. C., 2008. *Superlattices and Microstructures, 43 (5-6)*, 626-634.

Stöber W., Fink A., and Bohn E., 1968. *J. Colloid Interface Sci.,26*, 62.

Sheng-Li Chen, Peng Dong, Guang-Hua Yang, 1997. *Journal of Colloid and Interface Sci., 189* (2), 268–272.

Abderrafi Kamal, Jimenez Ernesto, Ben T., Molina S. I., Ibáñez R., Chirvony V., Martínez-Pastor J. P., 2012. *J. Nanoscience and Nanotechnology, 12* (8), 6774-6778.

Basudeb Karmakar, Goutam De, Dibyendu Ganguli, 2000. *Journal of Non-Crystalline Solids, 272*, 119–126.

Gijs van Soest and Ad Lagendijk, 2002. *Physical Review E, 65*, 047601.

Noginov M. A., Caulfield H. J., Noginova N. E., Venkateswarlu P., 1995. *Optics Communications, 118,* 430-437.

Yang Zhang, Yongsheng Chen, Paul Westerhoff, Kiril Hristovski, John C Crittenden, 2008. *Water Research, 42* (8-9), 2204–2212.

Chih-ping Tso, Cheng-min Zhung, Yang-hsin Shih, Young-Ming Tseng, Shian-chee Wu and Ruey-an Doong, 2010. *Water Science & Technology, 61* (1), 127-133.

van G., Wold A., 1993. *Chem. Mater., 5*, 280.

Amy L. Linsebigler, Guangquan Lu, and John T. Yates, 1995. Jr. *Chem. Rev., 95*, 735-758.

Serpone, N., Pelizzetti, E., 1989. "Photocatalysis-Fundamentals and Applications", Eds.; Wiley: *New York Chapter 7*, van Damme, H. *Supports in Photocatalysis*.

Tsukamoto M., Abe N., Soga Y., Yoshida M., Nakano H., Fujita M., Akedo J., 2008. *Appl Phys A, 93*, 193–196.

Heinz Ceriscber and Adam Heller, 1991. *The Journal of Physical Chemistry, 95* (13), 5261.

Tsukamoto Masahiro, Shinonaga Togo, Takahashi masanari, Fujita Masayuki,· Abe Nubuyuki, 2011. *Transactions of JWRI, 40* (1), 21-23.

Tsukamoto M., Abe N., Soga Y., Yoshida M., Nakano H., Fujita M., Akedo J., 2008. *Appl Phys A, 93*, 193–196.

Adrian Dunne and Michael F. Quinn, 1976. *J. Chem. Soc., Faraday Trans. 1, 72*, 2289-2295.

Yamashita, M.; Kashiwagi, H., 1976. *IEEE Journal of Quantum electronics,* 12 (1) Part:1, 90-95.